

Microlens Arrays by Direct-Writing Inkjet Print for LCD Backlighting Applications

Chung-Hao Tien, Chien-Hsiang Hung, and Tsung-Han Yu

Abstract—In this paper, we demonstrated the Inkjet print method to fabricate a ultraviolet (UV)-curable epoxy microlens deflecting array with controllable curvature and filling factor, by which a 7-in light guide plate with 82% uniformity and 70% light efficiency was successfully implemented. The microlenses can be directly formed by plastic discharged by inkjet head, eliminating the need for molds and slashing development time. Proposed method will certainly has a promising impact on rapid prototyping and other specialized microfeatures due to its simplicity and versatility.

Index Terms—Backlights, inkjet print, light guide plate, microlens array.

I. INTRODUCTION

BACKLIGHTING technology for the liquid-crystal displays (LCDs) has aimed to offer a planar luminance associated with uniform angular and spatial distribution. One of the key component of the backlight unit is the light guide plate (LGP), which converts a linearly side source, such as a cold cathode fluorescent lamp (CCFL) into the planar form. In the typical designs, the light guides have an irregular dot patterns on the bottom surface, as illustrated in Fig. 1(a), where the scattering kernel serves to spread the incident rays from the source over a wide angle to couple rays out from the LGP and obtain the brightness uniformity on the front surface. In order to improve the extraction efficiency or directivity, there have been several proposals to replace the conventional diffusing white spots by the carefully designed micro-features. The most common scheme was prismatic structure on the bottom of LGP to redirect the guided light out of the LGP within a narrow angular distribution [1], [2]. In addition to the prismatic configuration, the feature of microlens array (MLA) is another enabling structure for the customized characteristics of deflecting behavior, which yields a higher efficiency than the pure diffusing mechanism, as shown in Fig. 1(b). However, either micro-line prism or lens array is unlikely to *in-situ* modulate

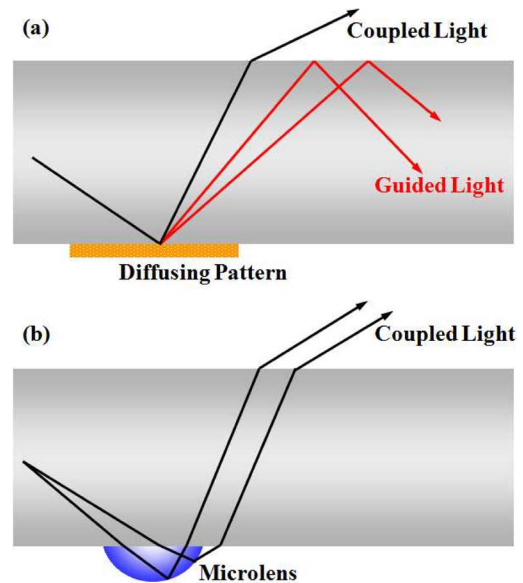


Fig. 1. Optical properties of: (a) conventional diffusing pattern and (b) microlens deflector.

the profile and arrangement by the general fabrication process such as diamond micromachining or lithography with injection molding or imprint technology. For this perspective, several rising technologies, like laser engraving [3], particle mixing [4], and inkjet printing [5], [6] are relatively advantageous to form the complex optical microstructure in terms of flexibility, accuracy, and cost.

Inkjet printing process is a kind of non-contact dot-matrix printing technology in which droplets of ink are jetted from a small aperture directly to a specified position on a substrate to create microfeatures, and widely applied in the field of defined polymer deposition, such as polymer light-emitting diode (PLED), organic thin film transistor (OTFT) and color filter, etc., [7], [8]. In this paper, we presented the use of this technology by utilization of a multi-nozzle inkjet printhead to implement a 7-in light guide plate. We investigated the printing process by the in-house developed UV curable epoxy/acrylate and demonstrated how to use microlens array for rapid prototyping in the display manufacture.

II. EXPERIMENT OF INK FORMATION

The microjet printing system can be divided into three critical components: the head, the substrate, and the inks. Strong correlation between these three factors mainly determines the quality of microlens and the subsequent performance [9], [10]. In this study, an automatically dropping device from Ulvac

Manuscript received September 02, 2008; revised November 24, 2008. Current version published April 01, 2009. This work was supported by the Ulvac Company, and by the National Science Council, Taiwan, for promoting academic excellence of the university in Photonics Science and Technology for Tetra Era under Grant NSC97-221-E-009-114-MY3.

C. H. Tien is with the Department of Photonics and Display Institute, National Chiao-Tung University, Hsinchu 30010, Taiwan (e-mail: chtien@mail.nctu.edu.tw).

C. H. Hung and T. H. Yu are with the Department of Photonics and Institute of Electro-Optical Engineering, National Chiao-Tung University, Hsinchu 30010, Taiwan.

Color versions of one or more of the figures in this paper are available online at <http://ieeexplore.ieee.org>.

Digital Object Identifier 10.1109/JDT.2009.2013874

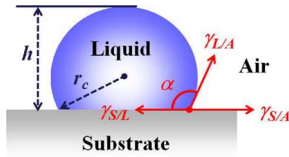


Fig. 2. Equilibrium of the surface tensions between liquid, substrate, and air.

(Litrex 70) was equipped. The system had a substrate holder, which can be moved in the X and Y directions with a long range of $20\text{ cm} \times 20\text{ cm}$. The piezoelectric-based print head, Spectra SE-128, manufactured from Fujifilm Dimatix, Inc., had a 128 individually addressed nozzle of $38\text{-}\mu\text{m}$ -diameter and was mounted on a carriage along the z -direction. Droplets were generated by changing the voltage across the piezoelectric actuator and holding it with a settled pulse width. The printing head allowed the user to determine the number of droplets to be deposited along the XY plane, and to ascribe a value to the spacing between every droplet. Two build-in charge-coupled device (CCD) modules were able to inspect the substrate condition and analyze the volume, velocity, and angle deviation of in-flight droplets *in situ*. All the operation can be well monitored by a graphical utility interface. UV-curable epoxy was a preferred class of material for the printing process due to its thermal and chemical durability. In order to enable the drop-on-demand printing, the viscosity of in-house developed UV curable epoxy/acrylate was reduced to below 20 cp at room temperature and to avoid nozzle clog. Meanwhile, the ejection frequency can be driven up to 1 kHz .

The shape of Inkjet microlens can be well controlled by the relation between the surface treatment of the substrate and the components of the ink, which include the binder, the monomer, and the photo initiator. In this case, the lens profile is designed as the spherical shape. Fig. 2 shows the schematic diagram of the lens cross section. The relation between the curvature and the contact angle θ in math can be started from the definition of the contact angle

$$h = r_c(1 - \cos \theta). \quad (1)$$

Here, h is the sag of the microlens, and r_c is the radius of curvature. Besides, the volume V of the spherical ink is calculated to be

$$V = \pi h^2 \frac{(3r_c - h)}{3} \quad (2)$$

where the lens sag is related to the radius of curvature and the contact angle by basic geometrical considerations. In this case, the relation between the curvature and the contact angle is derived from (1) and (2), as

$$r_c^3 = \frac{3V}{\pi(1 - \cos \theta)^2(2 + \cos \theta)}. \quad (3)$$

From the formula, the curvature is simultaneously defined by the contact angle and the ink volume. Here the ink volume can be generated by controlling the voltage of the print head. Besides, the contact angle is related to the surface wetting behavior.

To study the influence of the surface wetting behavior, a polymethyl-methacrylate (PMMA) substrate with different surface

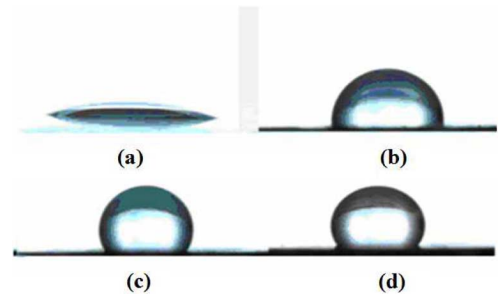


Fig. 3. Lens shape on the PMMA with various surface treatments. (a) dummy surface. (b) Hydrophobic surface. (c) Low-power RIE surface. (d) High-power RIE surface.

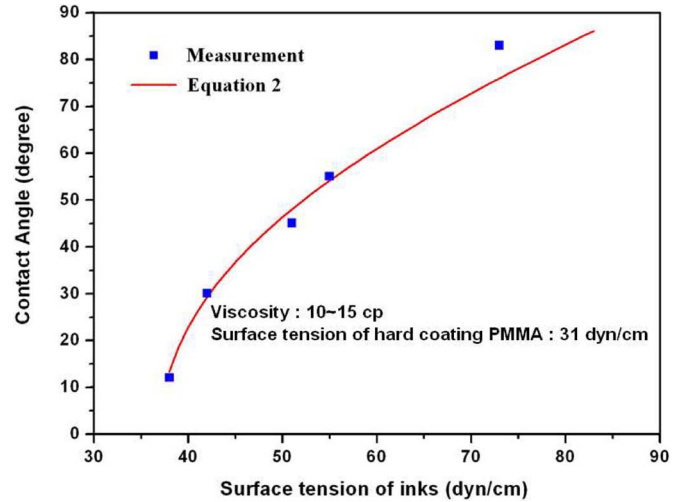


Fig. 4. Dependence of contact angle on the surface tension of ink, where the measurement results are in close agreement with the theoretical curve.

treatment were firstly discussed. The surface tension between the liquid, substrate, and environment mainly affects the shape of microlens, as shown in Fig. 2. The contact angle (α) in equilibrium for the ink droplet on various surface treatments is relevant to the interfacial tension, from Young's equation [11]

$$\gamma_{S/A} = \gamma_{S/L} + \gamma_{L/A} \cos \alpha. \quad (4)$$

where $\gamma_{S/A}$, $\gamma_{S/L}$, and $\gamma_{L/A}$ are the interfacial tension between each interface of the air, the liquid, and the substrate, respectively. Fig. 3 exhibits the experimental contact angles between a reference water droplet and the PMMA substrate with four surface treatments: (a) dummy surface; (b) hydrophobic treatment; (c) low-power etched surface via reactive ion etching; and (d) high-power etched surface. It is noted that hydrophobic treatment would increase $\gamma_{S/L}$ and resulted in a higher aspect ratio than the dummy surface. Moreover, etched treatment via reactive ion etching would further increase the interfacial tension and make contact angle higher than 90 degree. To evaluate those parameters related to the surface free energy, (5) can be derived from Young's equation as follows:

$$\gamma_{L/A}(1 + \cos \alpha) = 2(\gamma_{L/A}\gamma_{S/A})^{1/2} e^{-\beta(\gamma_{L/A} - \gamma_{S/A})^2} \quad (5)$$

where β is an empirical constant with an average value of $1.06 \times 10^{-4} (\text{m}^2\text{mJ}^{-1})^2$ [12]. The surface tension $\gamma_{S/A}$, of

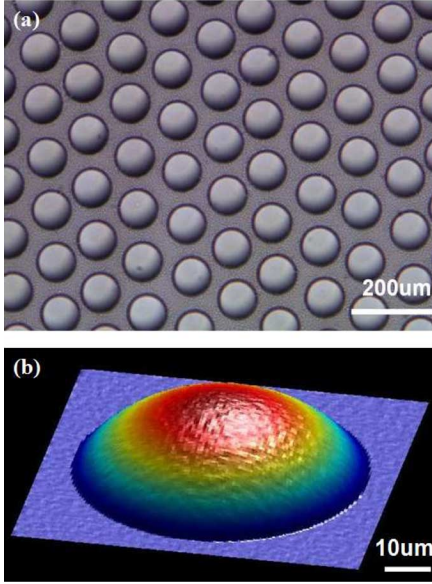


Fig. 5. (a) Microscopic photograph and (b) 3D interference profile of a single inkjet printed microlens.

the PMMA with perfluorine hard coating, which is so-called hydrophobic treatment, is substantially adopted as 31 dyne/cm, measured by a Paul N. Gardner contact angle detector. Thus, the dependence of the contact angle on the surface tension of inks can be predicted before the fabricating process. Fig. 4 showed the dependence of contact angle on the surface tension of ink, where the experimental results are in close agreement with the theoretical curve.

Based on the formation of droplets on the PMMA substrate, a deflecting microlens array (MLA) was able to be produced in high throughput. Thousands of droplet were jetted by a single nozzle within 1 s, thus a $20 \times 20 \text{ cm}^2$ substrate can be printed associated with desired patterns within a few seconds. After the printing process, the MLA was appropriately exposed under a 365-nm ultraviolet dose. Fig. 5 shows the microscopic photograph and 3-D interference profile of the microlens, where the MLA in a range of diameter $50 \pm 4 \text{ }\mu\text{m}$, sag $5 \pm 0.5 \text{ }\mu\text{m}$ and radius of curvature $65 \text{ }\mu\text{m}$ was obtained.

III. OPTICAL DESIGN

As the light energy from the light source was coupled into the LGP, the guided rays refracted and reflected by the MLA would destroy the total internal reflection (TIR), the uniformity and extraction efficiency can be adjusted by the desirable spherical pattern and arrangement. The configuration of overall backlighting unit was schematically shown in Fig. 6, where the UV-curable epoxy MLA was printed on the bottom surface of the LGP, combined with a white reflector. In order to meet the commercial angular distribution, additional low haze diffuser and prismatic sheets were placed above the LGP. In order to facilitate the design flow, the LGP in 7-inch was segmented into 10×10 divisions, where an optimum lens layout in each partition was calculated with modulated pitch subject to the identical lens shape. The extraction efficiency of an arbitrary unit cubic ($\eta = \Phi_E / \Phi_I$) was defined and shown in Fig. 7. Here Φ means

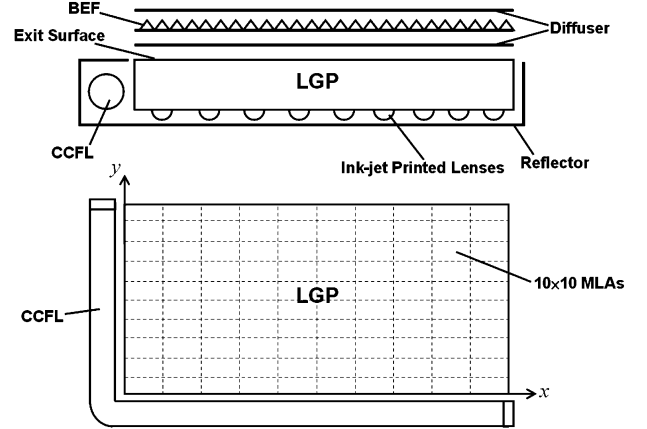


Fig. 6. UV-curable epoxy MLA was printed on the bottom surface of the light guide plate, combined with a white reflector. In addition, low haze diffusing and prismatic sheets were placed above the LGP. In order to facilitate the design flow, the LGP in 7-inch was segmented into 10×10 divisions, where an optimum lens layout in each partition was calculated with modulated pitch subject to the identical lens shape.

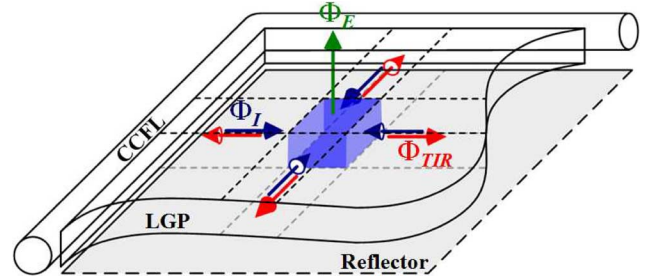


Fig. 7. Schematic diagram of light flux in an arbitrary unit. The incident flux is separated into extracted and guided parts.

the total flux through a single surface, and the subscripts, I , E , TIR and ABS mean the incident, extracted, guiding and absorbed light, respectively. According to energy conservation theory, the total flux through a spatial unit follows:

$$\Phi_I = \Phi_E + \Phi_{TIR} + \Phi_{ABS} \quad (6)$$

thus

$$\oint_{\text{unit}} M_I dA = \int_{\text{out plane}} M_E dA + \int_{\text{in plane}} M_{TIR} dA + \Phi_{ABS}. \quad (7)$$

M is the luminous emittance from a surface in consideration. Through the calculation by the Monte Carlo method, the extracting efficiency (η) in an arbitrary unit was found to be positively proportional to the filling factor of the microlens array, as shown in Fig. 8. The filling factor ascribed to the arrangement density was defined as $\rho = A_{\text{lens}} / A_{\text{unit}}$, where the A_{lens} is the occupied area of the lenses in a single unit A_{unit} . Thus, the illuminance analysis was conducted to evaluate the uniformity over the extracting surface by means of the identical flux unit. After incorporating the luminance function of CCFL and false position algorithm [13], the modulation of filling factor would optimize the uniformity at an appropriate angular extent for each partitioned unit.

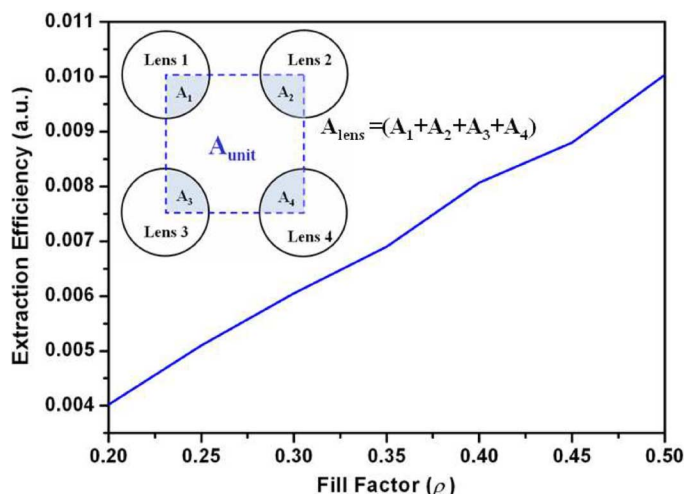


Fig. 8. Dependence of relative extraction efficiency on the fill factor of the MLA, where the A_{lens} is the occupied area of the lenses in a single unit A_{unit} . In this study, the fill factor was controlled in a range of 0.2–0.5.

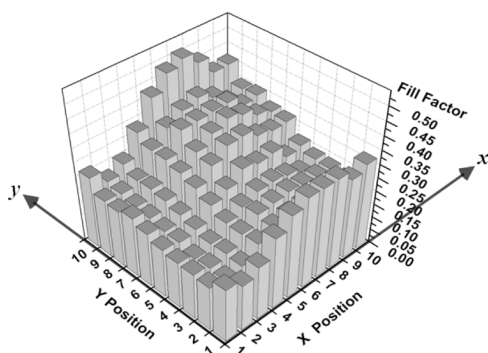


Fig. 9. Optimized fill factor distribution. Fill factor increases from the incident side.

IV. MEASUREMENT

The micrograph of the printed microlens array of a 7-in LGP was shown in Fig. 9, where the fill factor was ranged from 0.2 to 0.5 under 6% position errors. Fig. 10 shows the microscopic images of the microlens arrays with different fill factors. In order to characterize the UV-curable microlens array for backlighting, a commercially available optical module was equipped with the fabricated LGP. A photograph of the backlight module and the luminance distribution are shown in Fig. 11(a) and (b), respectively. The uniformity based on nine-point test, defined as $U = L_{\text{min}}/L_{\text{max}}$, was over 80% with average luminous 2500 nits. 70% light efficiency, defined as the ratio of the total flux emitted from the up surface over the total flux illuminating on the incident side of the LGP, was successfully implemented. Another examination of the UV-curable was the presence and magnitude of yellowness due to the influence of UV expose, where the exposure dose is 12500 mJ at 365-nm wavelength. The average color shift under the nine-point test was insignificant ($\Delta u'v' < 0.01$) in our case, which can be further reduced through the optimization of various experimental conditions.

V. SUMMARY

The capability of inkjet printing technology to print optical polymer for microlens array on a 7-inch light guide plate was

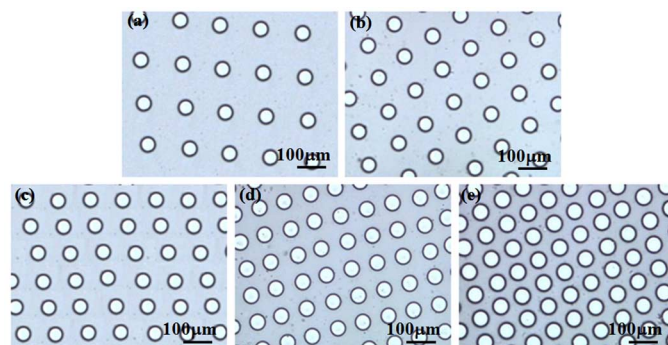


Fig. 10. Optical images of the fabricated MLA with different fill factor: (a) 0.2, (b) 0.25, (c) 0.3, (d) 0.4, and (e) 0.5. The position error of every microlens can be well suppressed down to 0.6%.

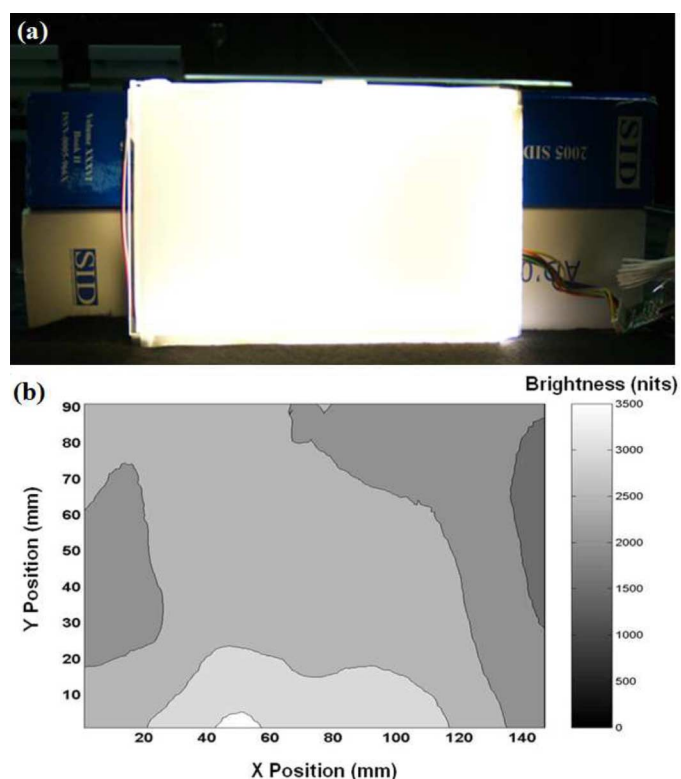


Fig. 11. (a) Photograph of the 7-in backlight module with inkjet printed MLA. (b) Average brightness was able to achieve 2500 nits with over 80% uniformity based on nine-point test.

demonstrated. We present our understanding of the characteristics of inkjet printing in the aspects of ink, print head and substrate. The microlens arrays by means of printing process exhibited several superiorities over traditional methods in terms of flexibility, accuracy and price. Moreover, this technology eliminates the need for molds and slashing development time from the standard six weeks to only about two days. Owing to direct writing, over 50% material consumption can be saved without sacrifice of optical performance. Proposed directly writing scheme will certainly provide opportunities both for significant cost reduction in existing light guide prototyping and for other optical features in the optoelectronic devices.

ACKNOWLEDGMENT

The support of the Litrex 70L inkjet printer from ULVAC Research Center, Taiwan, is acknowledged. The authors would like to thank Y.-H. Hsiau at AUO and Dr. J.-A. Cheng at National Chiao-Tung University, Hsinchu, Taiwan, for their technical assistance and discussion.

REFERENCES

- [1] K. Kälälantär, "Modified functional light-guide plate for backlighting transmissive LCDs," *J. SID*, vol. 11, no. 4, pp. 641–645, 2003.
- [2] C.-H. Tien, Y.-H. Lu, and Y.-J. Yao, "Tandem light-guides with micro-line-prism arrays for field-sequential-color scanning backlight module," *J. Display Technol.*, vol. 4, no. 2, pp. 147–152, Jun. 2008.
- [3] T. Kim, S. Park, H. Oh, and Y. Shin, "Analysis of the laser patterning inside light guide panel," *Optics & Laser Tech.*, vol. 39, pp. 1437–1442, 2007.
- [4] T. Okumura, A. Tagaya, and Y. Koike, "Highly-efficient backlight for liquid crystal display having no optical films," *Appl. Phys. Lett.*, vol. 83, pp. 2515–2517, 2003.
- [5] D. L. MacFarlane, V. Narayan, J. A. Tatum, W. R. Cox, T. Chen, and D. J. Hayes, "Microjet fabrication of microlens arrays," *IEEE Photon. Technol. Lett.*, vol. 6, no. 9, pp. 1112–1114, Sep. 1994.
- [6] P. Calvert, "Inkjet printing for materials and devices," *Chem. Mater.*, vol. 13, pp. 3299–3305, 2001.
- [7] B.-J. de Gans, P. C. Duineveld, and U. S. Schubert, "Inkjet printing of polymers: State of the art and future developments," *Adv. Mater.*, vol. 16, no. 3, pp. 203–213, 2004.
- [8] D. J. Hayes, M. E. Grove, D. B. Wallace, T. Chen, and W. R. Cox, "Inkjet printing in the manufacture of electronics, photonics, and displays," *Proc. SPIE*, vol. 4809, pp. 94–98, 2002.
- [9] B.-J. de Gans and U. S. Schubert, "Inkjet printing of well-defined polymer dots and arrays," *Langmuir*, vol. 20, pp. 7789–7793, 2004.
- [10] W. T. Pimbley and H. C. Lee, "Satellite droplet formation in a liquid jet," *IBM J. Res. Develop.*, vol. 20, no. 2, pp. 148–156, 1977.
- [11] D. M. Hartmann, O. Kibar, and S. C. Esener, "Optimization and theoretical modeling of polymer microlens arrays fabricated with the hydrophobic effect," *Appl. Opt.*, vol. 40, no. 16, pp. 2736–2746, 2001.
- [12] M. Gindl, G. Sinn, W. Gindl, A. Reiterer, and S. Tschegg, "A comparison of different methods to calculate the surface free energy of wood using contact angle measurements," *Colloids and Surfaces A*, vol. 181, pp. 279–287, 2001.
- [13] R. L. Burden and J. D. Faires, *Numerical Analysis*, 2000, Ed., 7th ed. Pacific Grove, CA: Brooks/Cole.

Chung-Hao Tien received the B.S. degree in communication engineering and the Ph.D. degree in electro-optical engineering from National Chiao Tung University, Hsinchu, Taiwan, in 1997 and 2003, respectively.

He joined National Chiao Tung University as an assistant professor at Department of Photonics and Display Institute since 2004 after as a post doctoral research staff at Carnegie Mellon University, Pittsburgh, PA. His current research interests are in optical data storage and non-imaging optics.

Chien-Hsiang Hung received the B.S. degree in physics from National Sun Yat-sen University, Kaohsiung, Taiwan, in 2004, and is currently working toward the Ph.D. degree in the Institute of Electro-Optical Engineering, National Chiao Tung University, Hsinchu, Taiwan.

His current researches are the optical design for non-image system and scattering optics.

Tsung-Han Yu received the B.S. degree in mechanical engineering and the M.S. degree in electro-optical engineering from National Chiao Tung University, Hsinchu, Taiwan, in 2006 and 2008, respectively.

Since 2008, he has been an engineer with Wellypower Optronics, Hsinchu Taiwan. His recently research is the optical design of LED luminaire.